The $[Co(NH_3)_5OH_2]^{3+}$ ion was chosen as an example of a substitutionally inert, unifunctional electrophile involving a first row transition metal ion. There is relatively little information on Co(III)-nucleotide complexes. Kistenmacher and Marzilli found that $[Co(acac)_2(NO_2)_2]^-$ reacted readily in aqueous solution with adenine but not cytosine, uracil, or guanine nucleotides to yield $[Co(acac)_2(NO_2)(dAdo)]$.[61] Coordination of deoxyadenosine was via N(7). With 25 mM *cis*-β-$[Co(trien)Cl_2]^+$ and ca. 10^{-4} M nucleosides, the following percent reaction values were obtained after 3 days in aqueous solution: dT, 65; dG, 50; dC, 10; dA, 0.[63] In the reaction between $[Co(NH_3)_5OH_2]^{3+}$ and the four-nucleo*tide* mixture, outer-sphere complexing with the phosphate is suggested by the visible spectrum, the lack of measurable perturbation of the Raman-active vibrations, and the products precipitated from more concentrated GMP and AMP solutions. Cleland and co-workers[33] obtained a species by reaction of $[Co(NH_3)_5OH_2]^{3+}$ in solution which they felt was $Co(NH_3)_5ADP$, although it could not be isolated or characterized. Coordination via the phosphate was tacitly assumed, although there was no proof of this.

(63) L. G. Marzilli, T. J. Kistenmacher, P. E. Darey, D. J. Szalda, and M. Beer, *J. Am. Chem. Soc.*, **96**, 4686 (1974).

Acknowledgments. We should like to thank Englehard Industries and Matthey Bishop, Inc., for loans of platinum. R. S. Tobias would like to thank the National Science Foundation for a NATO Senior Fellowship during the tenure of which a portion of this work was carried out. He also is indebted to Professor W. Beck of the University of Munich for Accommodations in his laboratory and many helpful discussions.

Supplementary Material Available: Raman spectra (6 pages). Ordering information is given on any current masthead page.

CIDNP-Detected Nuclear Resonance of Transient Radicals in Pulse Radiolysis

A. D. Trifunac* and W. T. Evanochko

Contribution from the Chemistry Division, Argonne National Laboratory, Argonne, Illinois 60439. *Received January 21, 1980*

Abstract: CIDNP detection of nuclear resonance in transient radicals produced by pulse radiolysis is described. CIDNP intensities of the reaction products can be perturbed by the application of radio frequency corresponding to the nuclear resonance in the transient radicals. In addition to the measurement of hyperfine coupling constants of transient radicals, the pulsed nature of the variable-field CIDNP nuclear resonance technique in pulse radiolysis can be used to measure radical kinetics and to study CIDEP population dynamics in various magnetic fields.

Introduction

The study of transient radical structure and dynamics in liquids has been a continuing challenge of magnetic resonance spectroscopy. While substantial improvements in the time-resolved EPR technique have been made,[1,2] ENDOR studies of transient radicals in solution have not yet been achieved. Nuclear resonance of transient radicals in liquids, however, can be detected via the CIDNP effect.[3] The CIDNP detected nuclear resonance experiment in variable magnetic fields is combined with the pulsed electron beam as a means of studying transient radicals.

The ease of observation of CIDNP in pulse radiolysis in both ^1H and natural abundance ^{13}C nuclei has been demonstrated.[4,5] In these experiments, the electron pulse irradiation is carried out in a variable magnetic field, and the reaction products are transferred to the NMR probe by using a fast flow system (Figure 1). The observation of CIDNP in various products of pulse radiolysis is possible because the transfer of the reaction products into the NMR probe is affected before appreciable nuclear spin relaxation takes place.

Here, we wish to illustrate further development of this experimental approach; where a radio frequency (rf) irradiation is supplied during the radical reaction in the variable magnetic field. When the appropriate radio frequency is applied during the radical lifetime, the electron nuclear spin populations of the transient radical are perturbed, resulting in a change of the CIDNP intensities in the radical reaction products.

The first demonstration of CIDNP-detected nuclear resonance was carried out by Sagdeev and co-workers.[3] In their experiments, radicals were produced by photolysis in the NMR probe. The continuous rf irradiation was carried out in the NMR probe itself. In the pulse radiolysis experiments to be discussed below, the pulsed nature of the excitation and the variable magnetic field of the reaction illustrates many new possibilities of the CIDNP-detected nuclear resonance in radicals.

The pulsed nature of the experiment allows the use of pulsed rf, thus high H_1 fields are available without the associated problems of sample heating. H_1 in the experiments to be described was in the 100-200-G range. Also, the pulsed nature of the experiment transforms what is an essentially steady-state CIDNP experiment into a time-resolved one, where time dependence, i.e., radical kinetics, of transient radicals can be studied. Furthermore, the rf power dependence of CIDNP-detected nuclear resonance (CIDNP-NR) allows differentiation of slower and faster radical pathways and thus CIDNP processes. The variable magnetic field allows the study of CIDNP-NR at all available fields (0-8 kG

(1) A. D. Trifunac and M. C. Thurnauer in "Time Domain Electron Spin Resonance", L. Kevan and R. N. Schwartz, Eds., Chapter 4, Wiley, New York, 1979, Chapter 4.
(2) (a) A. D. Trifunac and J. R. Norris, *Chem. Phys. Lett.*, **59**, 140 (1978); (b) A. D. Trifunac, J. R. Norris, and R. G. Lawler, *J. Chem Phys.*, **71**, 4380 (1979).
(3) (a) R. Z. Sagdeev, International Symposium on Magnetic Resonance in Chemistry, Biology and Physics (poster session), Argonne National Laboratory, Argonne, Illinois, June 1979; (b) R. Z. Sagdeev, Yu. A. Grishin, T. V. Leshina, A. Z. Gogolev, A. V. Dooshkin, and Yu. N. Molin, Abstracts, National Conference on the Advances of High-Resolution NMR Spectroscopy", Tashkent, U.S.S.R., 1979; (c) R. Z. Sagdeev, Yu. A. Grishin, A. Z. Gogolev, A. V. Dooshkin, A. G. Semenov, and Yu. N. Molin, *Zh. Strukt. Khim.*, **6** (1979).
(4) A. D. Trifunac and D. J. Nelson, *J. Am. Chem. Soc.*, **99**, 1745 (1977).
(5) R. G. Lawler, D. J. Nelson, and A. D. Trifunac, *J. Phys. Chem.*, (1979).

0002-7863/80/1502-4598$01.00/0

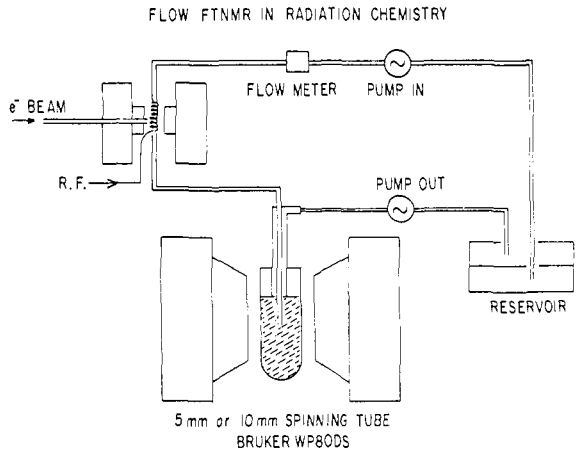

Figure 1. Schematic of the components of the CIDNP-NR experiment.

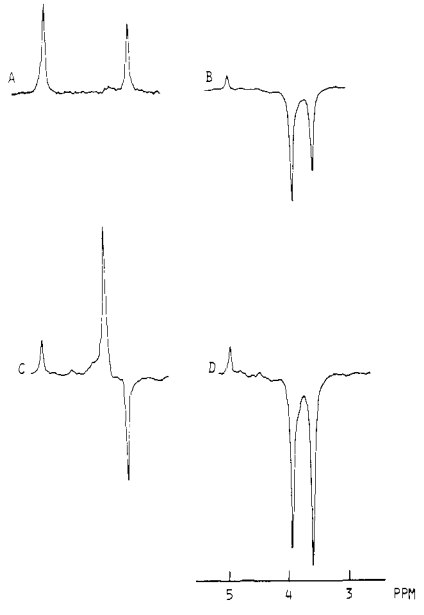

Figure 2. The CIDNP-NR effect in pulse radiolysis of 0.1 M methanol in D_2O at 100 G (methanol, 3.6 ppm; ethylene glycol, 3.9 ppm; HDO, 5.0 ppm): (A) without electron beam; (B) with electron beam; (C) B with rf at 30.000 MHz; (D) B with rf at 23.000 MHz.

in our case), allowing the study of field dependence of CIDEP by CIDNP detection.

Experimental Section

The schematic of the experimental setup is illustrated in Figure 1. During the radical lifetime (5–100 μs after the electron beam pulse), the radio frequency is turned on. In the kinetic runs, rf pulses as short as 1–2 μs were utilized. High H_1 fields were achieved by compact rf coil design and by utilizing a remotely tunable matching network. With H_1 typically in the 100–200-G range, a $\pi/2$ pulse would be 2–4 μs. The repetition rate of the electron beam pulse (3 MeV Van de Graaff) was typically 50 p/s. Typical electron beam widths were 100–500 ns. The irradiated solution was recirculated from the reservoir, where degassing with Ar or N_2O was carried out.

Results and Discussion

CIDNP-Detected Nuclear Resonance of the $\cdot CH_2OH$ Radical. The dominant reaction pathways in the pulse radiolysis of aqueous (D_2O) methanol are listed below in eq 1.[4] The CIDNP-NR effect

$$CH_3OD \xrightarrow{\cdot OD} \cdot CH_2OD \qquad (1)$$

$$2(\cdot CH_2OD) \rightarrow (CH_2OD)_2$$

$$\cdot CH_2OD + D\cdot \rightarrow CH_2DOD$$

$$e_{aq}^- + \cdot CH_2OD \rightarrow CH_2OD^- \xrightarrow{D^+} CH_2DOD$$

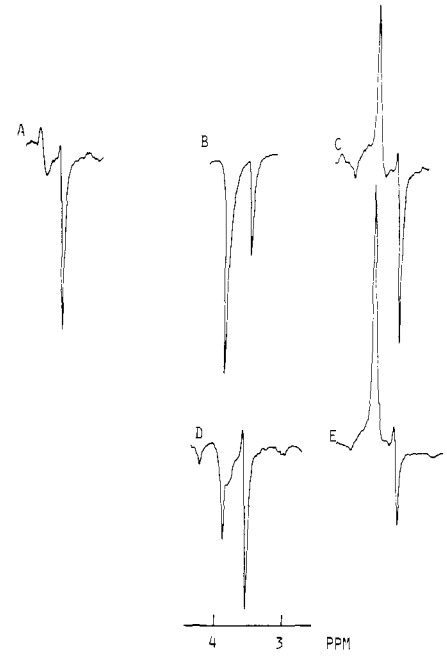

Figure 3. The CIDNP-NR effect in pulse radiolysis of 0.1 M methanol in D_2O at 1000 G: (A) with electron beam; (B) A with rf at 19.900 MHz; (C) A with rf at 20.700 MHz; (D) A with rf at 28.400 MHz; (E) A with rf at 29.300 MHz.

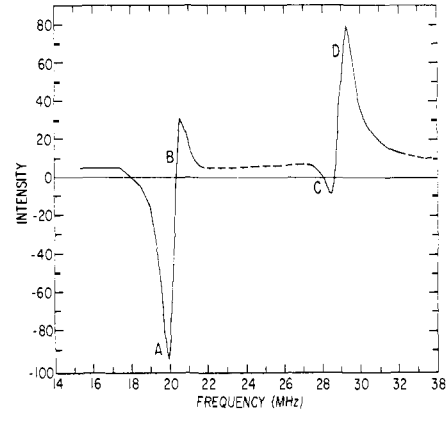

Figure 4. Transition widths of the CIDNP-NR effect of ethylene glycol at 1000 G illustrating second-order effects. Frequencies calcd/obsd: (A) 20.367/19.900 MHz; (B) 20.792/20.700 MHz; (C) 28.445/28.400 MHz; (D) 28.880/29.300 MHz (Note: observed frequencies have not been corrected for small differences due to the inaccuracy of the field setting).

is illustrated by the NMR spectra in Figures 2 and 3. What is immediately apparent is the considerable magnitude of the effect. At very low magnetic fields of the reaction ($\sim$100 G), H_1 is larger than the applied external magnetic field creating broad transition widths of the CIDNP-NR effect ($\sim$10 MHz). The second-order effects are quite visible in intermediate fields, e.g., 1000 G (Figure 4), and finally disappear at fields above 5000 G. The ease of observation of the CIDNP-NR effect depends on the ratio of CIDEP populations in the radical and the net effect in CIDNP of the same radical product. The CIDEP populations in the $\cdot CH_2OH$ radical are produced by the bimolecular reaction of the radical pairs involving two $\cdot CH_2OH$ radicals. This substantial E/A CIDEP can be easily observed by time-resolved EPR.[6] The CIDEP of the $\cdot CH_2OH$ radical makes no contribution whatsoever to the CIDNP of the products of the $\cdot CH_2OH$ radical (ethylene glycol and methanol) because no net population excess of nuclear spin states is created. The observed CIDNP emission in methanol and enhanced absorption in ethylene glycol, in magnetic fields

(6) A. D. Trifunac and M. C. Thurnauer, *J. Chem. Phys.*, **62**, 4889 (1975).

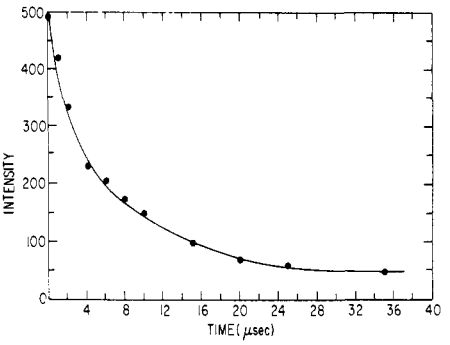

Figure 5. The time dependence of the CIDNP-NR signal intensity of ethylene glycol at 1000 G. (Note: the solid line is for illustrative purposes only).

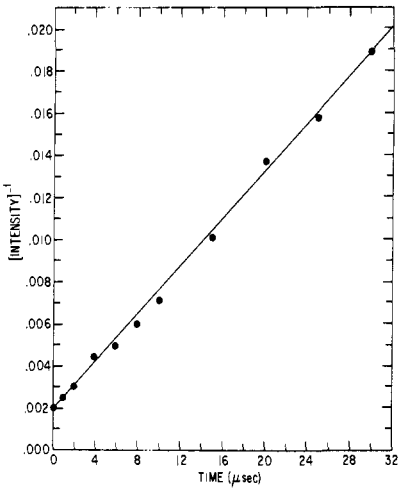

Figure 6. The CIDNP-NR signal intensity of ethylene glycol at 1000 G plotted as appropriate to second-order kinetics (Note: the solid line is for illustrative purposes only).

of the reaction of 1000 G or more, arise from the CIDNP polarization process involving an encounter of $\cdot CH_2OH$ and e_{aq}^- radicals giving rise to the "net" effect due to the substantial difference of the g factors of the two radicals. However, the substantial population difference in the electron nuclear states of the $\cdot CH_2OH$ radical can be transformed into a CIDNP observable population difference by the application of the radio frequency which induces nuclear transition in the radical electron nuclear spin states. The population differences arising in CIDEP are typically 2–10 times the electron spin Boltzman population ($\sim 10^{-3}$) of the radical.[6] These population differences for CIDEP are to be compared to the typical Boltzman population of ^1H in NMR ($\sim 10^{-6}$). Thus, even a small population transfer between the nuclear spin states of the transient radical can produce spectacular changes in the CIDNP of the radical product. Of course, when large CIDNP net effects are present (enhancement factors of several hundred or larger), the CIDNP-NR effect can become more difficult to observe. However, the ability to vary the magnetic field of the reaction as well as the reaction conditions allows one to adjust the ratio of CIDEP to CIDNP contribution as desired.

Further possible complications may arise from the electron-nuclear relaxation processes which are thought to be important in the intermediate magnetic fields ($\sim$1000–3000 G).[7]

(a) Hyperfine (a) Determination. As in the ENDOR experiment in the high-field limit, nuclear transitions in radicals occur at $a/2 \pm g_n\beta_nH_0$, where a is the hyperfine and $g_n\beta_nH_0$ is the nuclear Zeeman energy in the laboratory field H_0. In low fields and when second-order effects are present (depending on the a/H_0 ratio),

Figure 7. The CIDNP-NR effect in the pulse radiolysis of methanol–methyl iodide in D_2O at 1000 G: (A) with electron beam; (B) A with rf at 19.900 MHz; (C) A with rf at 36.500 MHz.

Breit-Rabi type formulas are used to calculate nuclear transition frequencies (e.g., Figure 4).[8] Actually, in low magnetic fields we can utilize a known radical (e.g., $\cdot CH_2OH$) with low-power rf pulse to calibrate the magnetic field.

(b) Radio Frequency Power Dependence and Radical Kinetics. In the course of our study, it became apparent that lower rf power was needed to effect slower reacting (longer lived) radicals. For example, in the methanol radiolysis glycol polarization can be influenced at very low rf power while even at the highest rf power available, the effect on methanol is always smaller. Thus, different radical lifetimes of the CIDNP cage product (methanol) vs. escape product (glycol) are differentiated.

Short rf pulses (~ 2 μs) are used to probe the time dependence of the CIDNP-NR signal intensity. The kinetic plots thus obtained are shown in Figures 5 and 6. The CIDNP-NR signal intensity vs. time of the rf pulse after the electron beam (at time zero) will represent true radical kinetics as long as the nuclear T_1 in radicals

(7) F. J. Adrian, H. M. Vyas, and J. K. S. Wan, *J. Chem. Phys.*, **65**, 1454 (1976).

(8) (a) G. Breit and I. I. Rabi, *Phys. Rev.*, **38**, 2082 (1931); (b) C. P. Poole and H. A. Farach, "The Theory of Magnetic Resonance", Wiley-Interscience, New York, 1972, p 203.

is appreciably longer than the chemical decay (second-order half-life) of radicals. This is the case with the $\cdot CH_2OH$ radical in the concentration range utilized ($\sim 10^{-3}$–10^{-4} M radical concentration/pulse). The plot (Figure 6) illustrates a second-order behavior of the $\cdot CH_2OH$ radical giving rise to ethylene glycol product. The $\cdot CH_2OH$ radical going to methanol product appears to have first-order behavior illustrating the different nature of the radical reaction pathway. Unfortunately, the methanol CIDNP-NR kinetic signal is appreciably more difficult to measure, and thus the scatter of kinetic points is considerable, as compared to glycol kinetics.

From the second-order plot (Figure 6) the second-order half-life of the $\cdot CH_2OH$ radical is ~ 6 μs. The radical concentration is evaluated to be $\sim 6 \times 10^{-4}$ M since the bimolecular rate constant for $\cdot CH_2OH$ is known ($(3 \pm 1) \times 10^8$ M^{-1} s^{-1}).[9] One can also obtain the radical concentration directly from the absorbed electron beam intensity. This latter approach yields a radical concentration of $\sim 10^{-3}$ M and a second-order rate constant of 1.6×10^8 M^{-1} s^{-1}. However, given the variables involved in the determination of the radical concentration, it is preferable to calibrate the experimental system by using a radical with a known second-order rate constant, as we have illustrated above. The accuracy of rate constants obtained by CIDNP-NR should compare quite favorably to those obtained by usual optical or fast EPR methods.[2b]

When the nuclear T_1 in radicals is equal to or faster than the second-order decay of radicals, a more complicated kinetic analysis utilizing a least-squares fitting to kinetic data will have to be used and the nuclear T_1 of radicals can thus be obtained.

Pulse Radiolysis of CH_3OH and CH_3I. CIDNP detected nuclear resonance in radicals can be used to provide a direct connection between the radicals and their fragments incorporated into reaction products. The radical system in the radiolysis of methanol–methyl iodide mixture in D_2O is used to illustrate this point (eq 2, Figure 7),[10] and the reactions of the $\cdot CH_2OD$ radical, eq 1, as in the methanol radiolysis.

$$CH_3I \xrightarrow{e_{aq}^-} \cdot CH_3 \qquad (2)$$

$$CH_3OD \xrightarrow{\cdot OD} \cdot CH_2OD$$

$$\cdot CH_2OD + \cdot CH_3 \rightarrow CH_3CH_2OD$$

$$2(\cdot CH_3) \rightarrow CH_3CH_3$$

$$\cdot CH_3 + \cdot D \rightarrow CH_3D$$

Figure 7A demonstrates the CIDNP spectrum obtained during the pulse radiolysis of an equimolar mixture of methanol and methyl iodide. The polarized products observed are methane (0.6 ppm), the methyl group of ethanol (1.6 ppm), methyl iodide (2.5 ppm), and the methylene group of ethanol (4.0 ppm). The weak emission at 3.1 ppm was not identified. When an rf of 19.900 MHz is applied (Figure 7B), only the products from the $\cdot CH_2OH$ fragment are affected. These signals are observed at 4.0 ppm, which illustrate the strong effect on the quartet from ethanol (ethylene glycol would also be within this intense signal), and at 3.6 ppm, which shows an emission for CH_2DOH not observed in Figure 7A. For a determination of which polarizations arise from the $\cdot CH_3$ radical, a radio frequency of 36.500 MHz is applied. The results which are shown in Figure 7C indicate the signals affected are methane at 0.6 ppm, which exhibits a slight increase in intensity, methyl iodide at 2.5 ppm, which shows complete inversion of its signal as compared to Figure 7A, and the triplet of methanol at 1.6 ppm, showing substantial increase in intensity. Interestingly, ethane is even observed at 1.2 ppm (weak enhanced absorption) which would have gone undetected in Figure 7A. In a more complex radical reaction system, where it may be less obvious what part of the radical product comes from which radical, this CIDNP-NR approach should prove a beneficial adjunct to the usual CIDNP study.

Summary and Further Comments

The detection of nuclear resonance in transient radicals in pulse radiolysis via the CIDNP effect has been illustrated. Experimentally this technique provides easy access to hyperfine coupling constants in transient radicals with accuracy similar to the ENDOR experiment. In addition, details of radical reaction mechanisms are obtainable either by the rf power dependence which allows differentiation between slower and faster radical processes or by relating the product fragment to the radical it came from. Furthermore, radical kinetics with 1–2 μs time resolution can easily be carried out. The quantitative details of CIDNP-NR transition widths and intensities can be used to study CIDEP in low and intermediate magnetic fields, a region that is so far unexplored. For example, the phase and relative intensity of the second-order nuclear transitions in Figure 4 suggest that the relative populations of the electron nuclear levels are such that the lowest levels in both upper and lower manifolds ($m_s = \pm 1/2$, $m_I = -1$ and 1) have larger populations than the middle levels ($m_s = \pm 1/2$, $m_I = 0$). Such relative population distribution is not obtainable from the CIDEP studies and, to our knowledge, has not been anticipated. Even details of electron nuclear and nuclear relaxation processes in transient radicals may be attainable by this approach. These possibilities are under investigation.

Acknowledgments. We wish to thank K. W. Johnson and B. E. Clifft for essential technical assistance. Useful discussions with Professor G. L. Closs, Professor R. G. Lawler, and Mr. J. A. Syage are acknowledged. We thank the Van de Graaff operators, R. H. Lowers and A. C. Youngs, for their efforts. Work was performed under the Office of Basic Energy Sciences, U.S. Department of Energy.

(9) Y. Ilan, J. Rabani, and A. Henglein, *J. Phys. Chem.*, **80**, 1558 (1976).
(10) J. W. T. Spinks and R. J. Woods, "An Introduction to Radiation Chemistry", 2nd ed., Wiley-Interscience, New York, 1976, p 397.